

1 **IgA autoantibodies target pulmonary surfactant in patients with severe COVID-19**

2

3 Tobias Sinnberg^{1,2*}, Christa Lichtensteiger^{3*}, Omar Hasan Ali^{3,4,5*}, Oltin T. Pop³, Mara Gilardi⁶,
4 Lorenz Risch^{7,8}, David Bomze^{3,9}, Philipp Kohler¹⁰, Pietro Vernazza¹⁰, Werner C. Albrich¹⁰, Christian
5 R. Kahlert^{10,11}, Silvio D. Brugger¹², Marie-Therese Abdou³, Carl Zinner⁶, Alexandar Tzankov⁶, Martin
6 Röcken^{1,2,13}, Lukas Kern¹⁴, Martin H. Brutsche¹⁴, Hubert Kalbacher¹⁵, Ana Velic¹⁶, Boris Maček¹⁶,
7 Josef M. Penninger^{5,17}, Matthias S. Matter⁶ & Lukas Flatz^{1,3,5,18}

8

9 * T.S., C.L., and O.H.A. contributed equally.

10

11 Affiliations:

12 1. Department of Dermatology, University Hospital Tübingen, Liebermeisterstraße 25, 72076
13 Tübingen, Germany

14 2. Cluster of Excellence iFIT (EXC 2180) Image Guided and Functionally Instructed Tumor
15 Therapies, University Hospital Tübingen, Liebermeisterstraße 25, 72076 Tübingen, Germany

16 3. Institute of Immunobiology, Kantonsspital St. Gallen, Rorschacher Strasse 95, 9007 St. Gallen,
17 Switzerland

18 4. Department of Medical Genetics, Life Sciences Institute, University of British Columbia, 2350
19 Health Sciences Mall, Vancouver V6T 1Z3, Canada

20 5. Department of Dermatology, University Hospital Zurich, University of Zurich, Rämistrasse 100,
21 8091 Zurich, Switzerland

22 6. Pathology, Institute of Medical Genetics and Pathology, University Hospital Basel, University of
23 Basel, Schönbeinstrasse 40, 4031 Basel, Switzerland

24 7. Labormedizinisches Zentrum Dr. Risch, Wuhrstrasse 14, 9490 Vaduz, Liechtenstein

25 8. Center of Laboratory Medicine, University Institute of Clinical Chemistry, University Hospital
26 Bern, University of Bern, INO-F, 3010 Bern, Switzerland

27 9. Sackler Faculty of Medicine, Tel Aviv University, P.O. Box 39040, Tel Aviv 6997801, Israel

1 10. Division of Infectious Diseases and Hospital Epidemiology, Kantonsspital St. Gallen,
2 Rorschacher Strasse 95, 9007 St. Gallen, Switzerland

3 11. Department of Infectious Diseases and Hospital Epidemiology, Children's Hospital of Eastern
4 Switzerland, Claudiusstrasse 6, 9000 St. Gallen, Switzerland

5 12. Department of Infectious Diseases and Hospital Hygiene, University Hospital Zurich, University
6 of Zurich, Rämistrasse 100, 8091 Zurich, Switzerland

7 13. German Cancer Research Consortium (DKTK), German Cancer Research Center (DKFZ), Im
8 Neuenheimer Feld 280, 69120 Heidelberg, Germany

9 14. Lung Center, Kantonsspital St. Gallen, Rorschacher Strasse 95, 9007 St. Gallen, Switzerland

10 15. Institute of Clinical Anatomy and Cell Analysis, University of Tübingen, Österbergstraße 3,
11 72074 Tübingen, Germany

12 16. Proteome Center Tübingen, Interfaculty Institute for Cell Biology, University of Tübingen, Auf
13 der Morgenstelle 15, 72076 Tübingen, Germany

14 17. Institute of Molecular Biotechnology of the Austrian Academy of Sciences (IMBA),
15 Dr.-Bohr-Gasse 3, 1030 Vienna, Austria

16 18. Department of Dermatology, Venereology and Allergology, Kantonsspital St. Gallen,
17 Rorschacher Strasse 95, 9007 St. Gallen, Switzerland

18

19 Corresponding author:

20 Prof. Lukas Flatz, MD

21 Department of Dermatology, University Hospital Tübingen, Liebermeisterstraße 25, 72076 Tübingen,
22 Germany; Phone: +49 7071 2984620; Email: lukas.flatz@med.uni-tuebingen.de

23

1 **ABSTRACT**

2 Complications affecting the lung are hallmarks of severe coronavirus disease 2019 (COVID-19).
3 While there is evidence for autoimmunity in severe COVID-19, the exact mechanisms remain
4 unknown. Here, we established a prospective observational cohort to study lung specific
5 autoantibodies (auto-Abs). Incubation of plasma from severe COVID-19 patients with healthy human
6 lung tissue revealed the presence of IgA antibodies binding to surfactant-producing pneumocytes.
7 Enzyme-linked immunosorbent assays (ELISA) and protein pull-downs using porcine surfactant
8 confirmed the presence of auto-Abs binding to surfactant proteins in severe COVID-19 patients. Mass
9 spectrometry and ELISAs with recombinant proteins identified IgA auto-Abs that target human
10 surfactant proteins B and C. In line with these findings, lungs of deceased COVID-19 patients showed
11 reduced pulmonary surfactant. Our data suggest that IgA-driven autoimmunity against surfactant may
12 result in disease progression of COVID-19.

1 INTRODUCTION

2 The Coronavirus disease 2019 (COVID-19), caused by infection with severe acute respiratory
3 syndrome coronavirus 2 (SARS-CoV-2), has rapidly evolved into a global pandemic with grave
4 socio-economic implications that affects every country worldwide.^{1,2} To date there have been reported
5 more than 100 million cases of infection with SARS-CoV-2 and over 2 million deaths across the
6 globe.³

7 While age and comorbidities have been established as predictors for clinical outcome,⁴ there is a lack
8 of validated factors that precede disease progression. Particular susceptibility factors, such as HLA
9 haplotype,⁵ blood type,⁶ and genetic polymorphisms of SARS-CoV-2 target receptors including
10 angiotensin converting enzyme 2 (ACE2)⁷ have been proposed. Yet, they are not utilized in standard
11 clinical management of COVID-19.⁸

12 Recent publications highlight a potential role of autoimmunity associated with COVID-19 severity, as
13 many patients develop symptoms that resemble autoimmune diseases, such as antiphospholipid
14 syndrome (APS), rheumatoid arthritis, and myositis.⁹⁻¹¹ Woodruff et al. have shown a surge of B-cell
15 responses that resemble those found in systemic lupus erythematosus (SLE) and further revealed that
16 high concentrations of neutralizing SARS-CoV-2 antibodies are associated with higher mortality.¹²

17 Bastard et al. reported that autoantibodies (auto-Abs) against the type I-interferons interferons (IFN)
18 $\alpha 2$ and IFN- ω inhibit the immune response against SARS-CoV-2, significantly increasing the
19 likelihood of disease progression.¹³ In line with these findings, an emerging report by Yang et al.
20 demonstrates that severely ill patients develop various auto-Abs against immunomodulatory proteins
21 that potentially perturb antiviral immune responses.¹⁴ Additionally, several studies have shown
22 significant elevations of APS-associated auto-Abs in severely ill patients, additionally explaining their
23 observed hypercoagulability and vascular inflammation.^{11,15} A further indication for the role of
24 autoimmunity is the significant reduction of mortality in severe and critically ill COVID-19 patients
25 by administration of dexamethasone,¹⁶ and preventing deterioration of disease using tocilizumab.¹⁷

26 Consequently, immunosuppression with dexamethasone has been widely established as standard
27 treatment of severe illness¹⁸ and other immunosuppressive drugs, such as colchicine and cyclosporine,
28 show benefits in preliminary study data.^{19,20}

1 While there is strong evidence for the role of autoimmunity in severe COVID-19, the exact
2 mechanisms have not been elucidated. Kanduc et al. have demonstrated amino acid sequence
3 similarities of the spike glycoprotein of SARS-CoV-2 and human surfactant-related proteins,
4 suggesting a cross-reactivity of immune responses due to antigen mimicry.²¹ Additional investigations
5 reveal a higher rate of shared protein epitopes between SARS-CoV-2 and the human proteome than
6 with other viruses, further supporting this finding.^{22,23} In a recent paper, Zuniga et al. have shown IgG
7 directed against annexin-2, a phospholipid-binding protein of the lung vasculature, is elevated in
8 severe COVID-19, indicating antibody cross-reactivity.²⁴ While autoimmune antibodies with cross-
9 reactivity have been proposed, a lung cell specific target has not yet been shown.

10 Here, we present that severe COVID-19 is significantly associated with an IgA-driven autoimmune
11 response that targets surfactant proteins in type 2 pneumocytes. This may result in diminished
12 surfactant and, thus, could drive progression of disease severity. We established a prospective
13 observational study and collected plasma samples of COVID-19 patients with varying disease
14 severity. Using immunofluorescence, we observed IgA bound to pulmonary surfactant in plasma of
15 only severely ill COVID-19 patients. We then performed enzyme-linked immunosorbant assays
16 (ELISAs) coated with poractant alfa, a natural surfactant extracted from porcine pulmonary tissue,
17 which revealed significant binding of immunoglobulins (Ig). By mass spectrometry, we were able to
18 identify surfactant proteins as candidate autoantigens. This was confirmed by ELISAs using
19 recombinant human surfactant proteins. Lastly, immunofluorescence of lung tissue of deceased
20 COVID-19 patients showed diminished surfactant. To summarize our findings, we identified IgA
21 auto-Abs targeting surfactant proteins which demonstrate IgA-driven autoimmunity, likely
22 contributing to compromised blood oxygenation. These data reveal an urgent need to explore the
23 preservation of surfactant proteins by immunosuppression and surfactant replacement in patients with
24 severe COVID-19.

25
26
27
28

1 RESULTS

2 Damaged lung tissue in COVID-19 shows autoimmune gene expression signatures

3 Most COVID-19 patients with fatal outcome develop diffuse alveolar damage (DAD), a life-threatening
4 destructive lung disease that leads to disturbed pulmonary function with reduced gas exchange.²⁵
5 Several pathologies, such as pulmonary edema, microthrombosis and fibrosis lead to respiratory
6 failure of patients with DAD. DAD from COVID-19 patients (COVID-19 DAD) show less
7 pronounced exudative changes and hemorrhages compared to non-COVID-19 DAD, as well as more
8 microthromboses, pulmonary thromboembolisms and new vessel growth (intussusceptive
9 angiogenesis), indicating additional drivers of pathology.²⁵⁻²⁷ In addition, COVID-19 is characterized
10 by an exaggerated immune response in the lung.²⁸ Thus, we hypothesized that the respiratory failure
11 of COVID-19 patients may be further aggravated by auto-Abs against self-antigens evoked by an
12 exaggerated immune activation. To understand if molecular pathways involved in autoimmunity are
13 present in lung tissue of severe COVID-19 patients (n=11), we performed gene expression analysis
14 with a panel specifically designed to analyze autoimmune disease (HTG EdgeSeq Immune Response
15 Panel). As a control group, we used patients with a DAD (n=10) caused by other reasons such as
16 drug-toxicity, lung surgery or myocardial infarction (**Fig. 1a; Supplementary Table 1**).
17 Unsupervised hierarchical clustering by *k*-means revealed clear grouping of COVID-19 patients and
18 non-COVID-19 patients in spite of both cohorts presenting with DAD (**Fig. 1b**). To explore, if
19 networks of autoimmune diseases are activated in COVID-19 patients, we performed gene set
20 enrichment analyses. To that end, we searched the Kyoto Encyclopedia of Genes and Genomes
21 database (KEGG; <https://www.genome.jp/kegg/pathway.html>) for autoimmune diseases and selected
22 “systemic lupus erythematosus (SLE)” and “autoimmune thyroid disease (ATD)”. To date, these
23 autoimmune diseases are the only ones in KEGG that entail a substantial production of auto-Abs.
24 While both pathways showed significant expression enrichment in lung tissue of COVID-19 autopsy
25 samples (**Fig. 1c**), only the enrichment compared to SLE remained significant after false discovery
26 rate (fdr)-adjustment (SLE normalized enrichment score: 1.6, $P=0.0008$, fdr-adjusted $P=0.02$; vs.
27 ATD normalized enrichment score: 1.9, $P=0.01$, fdr-adjusted $P=0.10$). In conclusion, these data show
28 that networks of autoimmune disorders with the production of auto-Abs are enriched in COVID-19

1 patients.

2

3 **Clinical study design**

4 In order to identify auto-Abs in patients with COVID-19 we enrolled N=46 individuals in a
5 prospective monocentric observational study and collected plasma samples. The median age was 61
6 years (interquartile range 55-70 years), and 32 (70%) were male. Patient characteristics are provided
7 in **Supplementary Table 2**. Patients were divided into subgroups by COVID-19 severity based on
8 clinical criteria.²⁹ In summary, we included 26 (57%) patients with critical, 13 (28%) with severe, and
9 7 (15%) with asymptomatic illness. For simplicity, patients with critical and severe disease will be
10 referred together as severe COVID-19. Additionally, we included plasma samples from healthy, non-
11 infected patients for control measurements. Details on patient recruitment are provided in the Methods
12 section.

13

14 **Autoimmune antibodies are elevated in severe COVID-19**

15 We assessed the presence of autoimmune-disease specific auto-Abs in COVID-19 patients and found
16 several auto-Abs that were elevated in individuals suffering from severe COVID-19 compared to
17 asymptomatic patients (**Fig. 1d**). Using the median antibody values of all cohorts, we calculated a
18 cumulative autoimmunity score (CAS). As expected, the CAS in severe COVID-19 patients was
19 significantly higher than in asymptomatic patients ($P=0.02$, two-tailed t-test, **Figure 1e**). In line with
20 the literature,¹⁴ our data showed elevated auto-Abs in severe COVID-19 compared to asymptomatic
21 patients, suggesting a vigorous auto-Abs response associated with disease severity.

22

23 **Severe COVID-19 patients develop autoantibodies against proteins in type II pneumocytes**

24 Given that we have detected autoimmune gene expression signatures, as well as auto-Abs, we next
25 determined the reactivity of auto-Abs in plasma samples from severe COVID-19 patients to any lung
26 protein using indirect immunofluorescence. Here, we inoculated plasma of severe COVID-19 patients
27 and healthy control patients with normal human alveolar lung tissue. We discovered specific binding
28 of IgA antibodies to distinguished areas of lung tissue (**Fig. 2a**). IgG were discoverable to a lesser

1 extent (**Supplementary Fig. 1**). Given that type II pneumocytes are the primary pulmonary target of
2 SARS-CoV-2,³⁰ we assessed mRNA expression from various lung alveolar cells using previously
3 published data.³¹ This revealed a characteristically high gene expression of surfactant proteins C
4 (SFTPC), B (SFTPB), A1 and A2 in type II pneumocytes (**Fig. 2b**). To examine, whether COVID-19
5 patients showed IgA and IgG derived autoreactivity against surfactant-producing cells, we performed
6 immunofluorescence and co-stained for surfactant protein A as a surrogate marker for type II
7 pneumocytes. This showed strong co-localization of IgA and surfactant (**Fig. 2c**), and, to a lesser
8 extent, of IgG and surfactant (**Supplementary Fig. 2**). Thus, our data indicate that predominantly IgA
9 auto-Abs bind to surfactant proteins in severe COVID-19 patients.

10

11 **IgA autoantibodies target surfactant protein B and C in patients with severe COVID-19**

12 In order to identify the target surfactant protein, we performed ELISA coated with poractant alfa.
13 Poractant alfa is an extract of porcine lung surfactant that consists of various phospholipids and
14 phospholipid-binding proteins, and is used as an intratracheal rescue therapy for infants with acute
15 respiratory lung distress syndrome (ARDS).³² ELISA results showed a significant presence of IgA
16 ($P=0.006$, Mann-Whitney U test, **Fig. 3a**) and IgG ($P=0.001$, **Supplementary Fig. 3**) directed against
17 poractant alfa in the plasma of severe COVID-19 patients compared to asymptomatic disease. Next,
18 we identified protein components of poractant alfa using mass spectrometry, which confirmed the
19 presence of SFTPB and SFTPC (**Fig. 3b**). To identify putative antigens, we prepared pull-down
20 affinity columns: here we used pooled and immobilized Ig from severe COVID-19 patients ($n=14$)
21 and uninfected healthy controls ($n=5$), after their incubation with poractant alfa. The extract was
22 analyzed by mass spectrometry to determine the Ig-captured proteins. Interestingly, SFTPB was the
23 most abundant protein with high enrichment (≥ 10 -fold) for captured proteins from plasma of severe
24 COVID-19 patients (**Fig. 3c**). Next, we used recombinant proteins of SFTPB and SFTPC to determine
25 the presence of autoreactive IgA and IgG in severe COVID-19 patients. The results showed a highly
26 significant difference of IgA against SFTPB (severe vs. asymptomatic, $P=0.001$, Mann-Whitney U
27 test) and for SFTPC (severe vs. asymptomatic, $P=0.004$) (**Fig. 3d**). Conversely, they showed no
28 significant difference for autoreactive IgG (**Supplementary Fig. 4**).

1

2 **Surfactant is diminished in lungs of deceased COVID-19 patients**

3 SARS-CoV-2 primarily infects cells via their angiotensin converting enzyme 2 (ACE2) receptors.³³
4 By infecting alveolar type II epithelial cells, which are rich in ACE2 receptors on their surface,
5 SARS-CoV-2 directly influences the function and production of surfactant proteins.³⁰ Our data of
6 auto-Abs against surfactant protein suggest an additional mechanism of surfactant disturbance. To
7 investigate, whether surfactant in lung tissue of COVID-19 patients is affected, we assessed its
8 presence in deceased COVID-19 patients with DAD and compared it to patients with non-COVID-19
9 DAD, and healthy controls. As suggested by previously reported gene expression analysis,³⁴ the total
10 amount of surfactant was reduced in COVID-19 patients in comparison to non-COVID-DAD as well
11 as to healthy controls (**Fig. 3e**).

12 In summary, we identified novel IgA-driven autoimmune response against SFTPB and SFTPC in
13 severe COVID-19 patients, which is associated with diminished surfactant. Our data suggest that a
14 vigorous B-cell response against self-antigens can corrupt crucial components for alveolar gas
15 exchange, possibly explaining progression of COVID-19 to ARDS. We suggest further mechanistic
16 exploration of this hypothesis.

17

18 **METHODS**

19 **Gene expression analysis:**

20 Samples were included based on quality control criteria by the manufacturer (HTG Molecular
21 Diagnostics, Tucson, AZ). These require that the percentage of overall reads allocated to the positive
22 process control probe per sample is less than 28%, the read depth is at least 750000 and the relative
23 standard deviation of reads allocated to each probe within a sample is greater than 0.094. In addition,
24 only samples with a known postmortem interval were preserved for differential analysis. Differential
25 expression analysis was conducted in R version 4.0.3 (R Project for Statistical Computing, Vienna,
26 Austria) with the DESeq2 package using default settings. Count estimates were normalized with the
27 median ratio method. Differential gene expressions for the contrast of COVID-19 patients with DAD
28 vs. control patients with other DAD were modelled with a negative binomial distribution and

1 subjected to a Wald significance test. Prior to heatmap visualization, the normalized counts were
2 further \log_2 transformed using a robust variance stabilization. The heatmap of genes with a $|\log$
3 fold change $| > 1$ was produced with the complexHeatmap package. Column sample clusters were
4 obtained by k-means clustering with $k = 2$ and row gene clusters by hierarchical clustering with
5 complete linkage. Functional analysis was quantified via gene set enrichment. All genes in the
6 autoimmune panel were pre-ranked using the Wald test statistic and submitted to the entire KEGG
7 database of human pathways using the clusterProfiler package.

8

9 **Clinical study: patient recruitment, data and blood sample collection**

10 Patient data and blood collection was approved by the Ethics committee of Eastern Switzerland (study
11 ID 2020-01006), and tissue collection by Ethics committee of Northern and Central Switzerland
12 (study ID 2020-00969). The studies were performed in accordance with the Declaration of Helsinki
13 guidelines.³⁵ Collection of patient data and samples (serum or plasma) was conducted from April 9,
14 2020, to May 1, 2020 and tissue collection from March 13 2020 to May 4 2020. SARS-CoV-2
15 infection of the severe COVID-19 cohort was confirmed by real-time reverse transcriptase-
16 polymerase chain reaction³⁶ of nasopharyngeal swab samples. Infection of asymptomatic COVID-19
17 was confirmed with serology of SARS-CoV-2 antibodies, using two independent antibody tests: SGIT
18 flex Covid 19, a lateral flow immunochromatographic assay (LFIA) (Sugentech, Daejeon, South
19 Korea), and Elecsys Anti-SARS-CoV-2, an electro-chemiluminescence immunoassay (ECLIA)
20 (Roche International Diagnostics AG, Rotkreuz, Switzerland). We defined a positive result as
21 elevated SARS-CoV-2 IgG in the LFIA in the acute phase with confirmation by IgG in the ECLIA
22 after 3-4 weeks. All blood samples of severe COVID-19 patients were obtained within the first two
23 weeks of symptom onset. Due to the unknown primary infection of patients with asymptomatic
24 COVID-19, blood draw at an unknown timepoint is assumed.

25

26 **Plasma isolation from whole blood**

27 Plasma samples were isolated from sodium-heparin whole blood (BD Vacutainer® CPT™ tubes,
28 Becton Dickinson, NJ). Briefly, the tubes were centrifuged at room temperature (RT) at 1650 g for 20

1 minutes at room temperature. The undiluted plasma was then aliquoted and stored at -80 °C for
2 subsequent analysis.

3

4 **Antibody analysis**

5 Myositis and systemic sclerosis antibodies (i.e. Mi-2a, Mi-2b, TIF1g, MDA5, NXP2, SAE1, Ku, PM-
6 SCL100, PM-SCL75, Jo-1, SRP, PL-7, PL-12, EJ, OJ, Ro5 for myositis; Scl-70, CENPA, CENPB,
7 RP11 (RNAP-III), RP155 (RNAP-III), Fibrillarin, NOR-90, Th/To, PM-Scl100, PM-Scl175, Ku,
8 PDGRF, Ro-52 for systemic sclerosis) were determined via immunoblot using the EuroBlotOne test
9 system (Euroimmun AG, Lübeck, Germany), respectively, following the manufacturer's instructions.
10 Autoantibodies against Cardiolipin, β -2-glycoprotein 1, double stranded DNA (dsDNA), cyclic
11 citrullinated peptide (CCP), SSA1, SSA2, SSB, Sm, PR3, and MPO were determined by fluorescence
12 enzyme immunoassay on a Unicap 250 analyzer (Thermo Fisher Scientific, Waltham, U.S.A.).
13 Rheumatoid factor (RF) was determined by turbidimetry (COBAS 6000, Roche Diagnostics,
14 Rotkreuz, Switzerland). Measurements were performed at the Labormedizinisches Zentrum Dr. Risch
15 (Buchs, St. Gallen, Switzerland), an ISO 17025:2018 accredited medical laboratory. The cumulative
16 autoimmunity score (CAE) for each patient was generated in two steps: First, we calculated the
17 median value of all the analyses results of a given autoantibody. Second, we determined for each
18 patient, if the result is above (score of "1") or below (score of "0") that value. The CAE represents the
19 sum of those scores across all autoantibodies for any given patient.

20

21 **Indirect immunofluorescence**

22 Four serial frozen sections from 4 lung tissues from patients without COVID-19 infection were
23 washed two times with PBS 0.1% Tween 20, for 5 min each. In a first step one section from each lung
24 tissue was then incubated for 30 minutes at RT with plasma from severe COVID-19 patients (plasma
25 pooled from three patients and diluted 1:3 in PBS), and another with serum from healthy donors
26 (pooled from three individuals, diluted 1:3 in PBS), and two slides with PBS only (negative controls).
27 After washing, one of the of the control slides was then incubated with sterile PBS for 30 min at room
28 temperature, while the remaining three slides were incubated with anti-IgA FITC (Dako, catalog no.

1 F0204; dilution 1:50) or anti-IgG FITC (Dako, catalog no. F0202; dilution 1:50) for 30 minutes at RT.
2 Slides were then counterstained with DAPI (ThermoFisher, catalog no. D1306) and mounted using
3 fluorescence mounting medium (Dako, catalog no. S3023). Slides were imaged and assessed using a
4 Zeiss LSM 710 laser scanning microscope (Carl Zeiss AG, Oberkochen, Germany).

5

6 **Co-localization immunofluorescence staining**

7 Fresh frozen lung tissues were incubated with the above described patients' plasma pools diluted 1:3
8 for 30 min RT. Immunofluorescence staining was performed as previously described.³⁷⁻³⁹ Briefly,
9 anti-surfactant (diluted 1:100 ab51891, Abcam), anti-IgA FITC and anti-IgG FITC primary antibodies
10 (diluted 1:50, respectively F0316-F0202 Dako) were used. Then, the incubation with the serum
11 secondary antibody alexa-fluor 647 (Invitrogen) was done. DAPI incubation for 10 minutes has been
12 performed to stain the nuclei. Samples were mounted in prolong gold anti-fade mounting medium
13 (Invitrogen) and scanned by confocal microscope (Ti2, Nikon, Tokyo, Japan). Images were analyzed
14 using QuPath software⁴⁰ as previously reported.³⁷ Intensity fluorescence profile has been analyzed by
15 Nikon software to determine the co-localization of the signals as previously reported.³⁸

16

17 **SFTPb immunofluorescence staining**

18 We compared the presence of SFTPb in formalin-fixed paraffin-embedded lung tissues obtained from
19 deceased patients with COVID-19 DAD, non-COVID-19 DAD and normal lungs as controls. Tissues
20 were processed as previously described for immunofluorescence staining.³⁷⁻³⁹ Briefly, antigen
21 retrieval was performed, and tissues incubated with PBS 0.1% Tween-20. Staining using anti-SFTPb
22 antibodies diluted 1:100 (NCL-SPPB) was done in blocking buffer for 1h at RT. Alexa-fluor 647
23 (Invitrogen) was applied as secondary antibody. Controls for secondary antibody specificity were
24 generated by substituting the primary antibody with blocking buffer only. All samples were incubated
25 with DAPI for 10 minutes and mounted in prolong gold anti-fade mounting medium (Invitrogen) and
26 scanned with the Ti2 confocal microscope (Nikon, Tokyo, Japan).

27

1 **Single cell RNA data analysis**

2 Single-cell RNA sequencing data of healthy lungs were obtained from the LungMap project³¹ via the
3 ToppCell portal (<https://toppcell.cchmc.org/>). Counts were normalized to log₂-transcripts per million
4 (TPM) and compared across the 7 major epithelial cell types: type-1, and type-2 alveolar-, basal-,
5 ciliated-, club-, and goblet cells, as well as ionocytes. Housekeeping genes were excluded from the
6 analysis. Cell-specific genes were defined as those with overall expression log₂-TPM > 5 and at least
7 4-fold higher expression in one or two particular cell types compared to all other cell types.

8

9 **Immunoglobulin isolation from COVID-19 plasma samples**

10 Plasma samples from 14 critical/severe COVID-19 patients and 5 asymptomatic patients were pooled
11 and immunoglobulins were isolated from 1 ml each of the plasma pools using 4 mL protein L coupled
12 agarose resin (Capto™ L, Cytiva Life Sciences, Amersham, UK) packed into 15 mL empty
13 polypropylene columns (Chromabond, Machery-Nagel, Düren, Germany). After extensive washing
14 with PBS-T (0.05% Tween 20) the immunoglobulins were eluted in 0.1 M glycine buffer pH 2.5. 50
15 % of the isolated immunoglobulins from the pools were individually and chemically cross-linked onto
16 1 g of CNBr-activated sepharose (CNBr-activated Sepharose® 4B, Cytiva) as recommended by the
17 manufacturer and packed into 15 mL empty polypropylene columns (Chromabond, Machery-Nagel).
18 The protein content of 0.33 mL Curosurf® (poractant alfa, Chiesi Farmaceutici, Parma, Italy) was
19 immuno-purified after acetone precipitation in 15 mL of PBS-T per column by overnight binding at
20 4°C using a peristaltic pump (ISM597A, Ismatec, Wertheim, Germany) and a circuit flow rate of 0.5
21 mL/min, washing with 100 ml of PBS-T and elution in glycine buffer pH 2.5.

22

23 **Protein identification by mass spectrometry**

24 A SDS PAGE short gel purification was run with either acetone-precipitated 0.2 mL Curosurf® or the
25 immuno-purified and eluted proteins and in-gel digestion with Trypsin was conducted as described
26 previously.⁴¹ Extracted peptides were desalted using C18 StageTips⁴² and subjected to LC-MS/MS
27 analysis. LC-MS/MS analyses were performed on an Easy-nLC 1200 UHPLC (Thermo Fisher
28 Scientific, Waltham, MA) coupled to an QExactive HF Orbitrap mass spectrometer (Thermo Fisher

1 Scientific) as described elsewhere,⁴³ or an Orbitrap Exploris 480 mass spectrometer (Thermo Fisher
2 Scientific) as previously described.⁴⁴ Peptides were eluted with a 60 min segmented gradient at a flow
3 rate of 200nl/min, selecting 20 most intensive peaks for fragmentation with HCD. The MS data was
4 processed with MaxQuant software suite v.1.6.7.0⁴⁵ to measure the iBAQ which was used to calculate
5 the relative protein level ($riBAQ=iBAQ/(\sum iBAQ)$). Database search was provided against pig
6 (121817 entries) and human (96817 entries) UniProt database using the Andromeda search engine.⁴⁶
7

1 REFERENCES

- 2 1 Townsend, E. COVID-19 policies in the UK and consequences for mental health. *Lancet*
3 *Psychiatry* **7**, 1014-1015, doi:10.1016/S2215-0366(20)30457-0 (2020).
- 4 2 Lane, H. C. & Fauci, A. S. Research in the Context of a Pandemic. *N Engl J Med*,
5 doi:10.1056/NEJMe2024638 (2020).
- 6 3 John Hopkins University. *Coronavirus Resource Center*,
7 <<https://coronavirus.jhu.edu/map.html>> (2020).
- 8 4 Wiersinga, W. J., Rhodes, A., Cheng, A. C., Peacock, S. J. & Prescott, H. C.
9 Pathophysiology, Transmission, Diagnosis, and Treatment of Coronavirus Disease 2019
10 (COVID-19): A Review. *JAMA* **324**, 782-793, doi:10.1001/jama.2020.12839 (2020).
- 11 5 Nguyen, A. *et al.* Human Leukocyte Antigen Susceptibility Map for Severe Acute
12 Respiratory Syndrome Coronavirus 2. *J Virol* **94**, doi:10.1128/JVI.00510-20 (2020).
- 13 6 Severe Covid, G. G. *et al.* Genomewide Association Study of Severe Covid-19 with
14 Respiratory Failure. *N Engl J Med* **383**, 1522-1534, doi:10.1056/NEJMoa2020283 (2020).
- 15 7 Hou, Y. *et al.* New insights into genetic susceptibility of COVID-19: an ACE2 and
16 TMPRSS2 polymorphism analysis. *BMC Med* **18**, 216, doi:10.1186/s12916-020-01673-z
17 (2020).
- 18 8 World Health Organization (WHO). *Clinical management of COVID-19*, 27 May 2020,
19 <<https://apps.who.int/iris/rest/bitstreams/1278777/retrieve>> (2020).
- 20 9 Malas, M. B. *et al.* Thromboembolism risk of COVID-19 is high and associated with a higher
21 risk of mortality: A systematic review and meta-analysis. *EClinicalMedicine* **29**, 100639,
22 doi:10.1016/j.eclinm.2020.100639 (2020).
- 23 10 Vlachoyiannopoulos, P. G. *et al.* Autoantibodies related to systemic autoimmune rheumatic
24 diseases in severely ill patients with COVID-19. *Ann Rheum Dis* **79**, 1661-1663,
25 doi:10.1136/annrheumdis-2020-218009 (2020).
- 26 11 Hasan Ali, O. *et al.* Severe COVID-19 is associated with elevated serum IgA and
27 antiphospholipid IgA-antibodies. *Clin Infect Dis*, doi:10.1093/cid/ciaa1496 (2020).

- 1 12 Woodruff, M. C. *et al.* Extrafollicular B cell responses correlate with neutralizing antibodies
2 and morbidity in COVID-19. *Nat Immunol* **21**, 1506-1516, doi:10.1038/s41590-020-00814-z
3 (2020).
- 4 13 Bastard, P. *et al.* Autoantibodies against type I IFNs in patients with life-threatening COVID-
5 19. *Science* **370**, doi:10.1126/science.abd4585 (2020).
- 6 14 Wang, E. Y. *et al.* Diverse Functional Autoantibodies in Patients with COVID-19. Preprint at
7 <https://www.medrxiv.org/content/10.1101/2020.12.10.20247205v5> (2020).
- 8 15 Zuo, Y. *et al.* Prothrombotic autoantibodies in serum from patients hospitalized with COVID-
9 19. *Sci Transl Med* **12**, doi:10.1126/scitranslmed.abd3876 (2020).
- 10 16 Horby, P. *et al.* Dexamethasone in Hospitalized Patients with Covid-19 - Preliminary Report.
11 *N Engl J Med*, doi:10.1056/NEJMoa2021436 (2020).
- 12 17 Salama, C. *et al.* Tocilizumab in Patients Hospitalized with Covid-19 Pneumonia. *N Engl J*
13 *Med* **384**, 20-30, doi:10.1056/NEJMoa2030340 (2021).
- 14 18 US Center for Disease Control (CDC). *COVID-19 treatment guidelines*,
15 <<https://www.covid19treatmentguidelines.nih.gov/therapeutic-management>> (2020).
- 16 19 Lopes, M. I. F. *et al.* Beneficial effects of colchicine for moderate to severe COVID-19: an
17 interim analysis of a randomized, double-blinded, placebo controlled clinical trial. Preprint at
18 <https://www.medrxiv.org/content/10.1101/2020.08.06.20169573v2> (2020).
- 19 20 Guisado-Vasco, P. *et al.* Clinical characteristics and outcomes among hospitalized adults with
20 severe COVID-19 admitted to a tertiary medical center and receiving antiviral, antimalarials,
21 glucocorticoids, or immunomodulation with tocilizumab or cyclosporine: A retrospective
22 observational study (COQUIMA cohort). *EClinicalMedicine* **28**, 100591,
23 doi:10.1016/j.eclinm.2020.100591 (2020).
- 24 21 Kanduc, D. & Shoenfeld, Y. On the molecular determinants of the SARS-CoV-2 attack. *Clin*
25 *Immunol* **215**, 108426, doi:10.1016/j.clim.2020.108426 (2020).
- 26 22 Kanduc, D. From Anti-SARS-CoV-2 Immune Responses to COVID-19 via Molecular
27 Mimicry. *Antibodies (Basel)* **9**, doi:10.3390/antib9030033 (2020).

- 1 23 Kanduc, D. & Shoenfeld, Y. Molecular mimicry between SARS-CoV-2 spike glycoprotein
2 and mammalian proteomes: implications for the vaccine. *Immunol Res* **68**, 310-313,
3 doi:10.1007/s12026-020-09152-6 (2020).
- 4 24 Zuniga, M. *et al.* Autoimmunity to the Lung Protective Phospholipid-Binding Protein
5 Annexin A2 Predicts Mortality Among Hospitalized COVID-19 Patients. Preprint at
6 <https://www.medrxiv.org/content/10.1101/2020.12.28.20248807v1> (2021).
- 7 25 Menter, T. *et al.* Postmortem examination of COVID-19 patients reveals diffuse alveolar
8 damage with severe capillary congestion and variegated findings in lungs and other organs
9 suggesting vascular dysfunction. *Histopathology* **77**, 198-209, doi:10.1111/his.14134 (2020).
- 10 26 Ackermann, M. *et al.* Pulmonary Vascular Endothelialitis, Thrombosis, and Angiogenesis in
11 Covid-19. *N Engl J Med* **383**, 120-128, doi:10.1056/NEJMoa2015432 (2020).
- 12 27 Borczuk, A. C. *et al.* COVID-19 pulmonary pathology: a multi-institutional autopsy cohort
13 from Italy and New York City. *Mod Pathol* **33**, 2156-2168, doi:10.1038/s41379-020-00661-1
14 (2020).
- 15 28 Nienhold, R. *et al.* Two distinct immunopathological profiles in autopsy lungs of COVID-19.
16 *Nat Commun* **11**, 5086, doi:10.1038/s41467-020-18854-2 (2020).
- 17 29 Gandhi, R. T., Lynch, J. B. & Del Rio, C. Mild or Moderate Covid-19. *N Engl J Med* **383**,
18 1757-1766, doi:10.1056/NEJMcp2009249 (2020).
- 19 30 Hu, B., Guo, H., Zhou, P. & Shi, Z. L. Characteristics of SARS-CoV-2 and COVID-19. *Nat*
20 *Rev Microbiol*, doi:10.1038/s41579-020-00459-7 (2020).
- 21 31 Vieira Braga, F. A. *et al.* A cellular census of human lungs identifies novel cell states in
22 health and in asthma. *Nat Med* **25**, 1153-1163, doi:10.1038/s41591-019-0468-5 (2019).
- 23 32 US Food and Drug Administration (FDA). *CUROSURF (poractant alfa) intratracheal*
24 *suspension*,
25 <https://www.accessdata.fda.gov/drugsatfda_docs/label/2014/020744s0281bl.pdf> (2020).
- 26 33 Monteil, V. *et al.* Inhibition of SARS-CoV-2 Infections in Engineered Human Tissues Using
27 Clinical-Grade Soluble Human ACE2. *Cell* **181**, 905-913 e907,
28 doi:10.1016/j.cell.2020.04.004 (2020).

- 1 34 Islam, A. & Khan, M. A. Lung transcriptome of a COVID-19 patient and systems biology
2 predictions suggest impaired surfactant production which may be druggable by surfactant
3 therapy. *Sci Rep* **10**, 19395, doi:10.1038/s41598-020-76404-8 (2020).
- 4 35 World Medical Association. *Declaration of Helsinki – Ethical Principles for Medical
5 Research Involving Human Subjects*, <[https://www.wma.net/policies-post/wma-declaration-
6 of-helsinki-ethical-principles-for-medical-research-involving-human-subjects/](https://www.wma.net/policies-post/wma-declaration-of-helsinki-ethical-principles-for-medical-research-involving-human-subjects/)> (2020).
- 7 36 Corman, V. M. *et al.* Detection of 2019 novel coronavirus (2019-nCoV) by real-time RT-
8 PCR. *Euro Surveill* **25**, doi:10.2807/1560-7917.ES.2020.25.3.2000045 (2020).
- 9 37 Gilardi, M. *et al.* Tipifarnib as a Precision Therapy for HRAS-Mutant Head and Neck
10 Squamous Cell Carcinomas. *Mol Cancer Ther* **19**, 1784-1796, doi:10.1158/1535-7163.MCT-
11 19-0958 (2020).
- 12 38 Banerjee, S. *et al.* Anti-KIT DNA Aptamer for Targeted Labeling of Gastrointestinal Stromal
13 Tumor. *Mol Cancer Ther* **19**, 1173-1182, doi:10.1158/1535-7163.MCT-19-0959 (2020).
- 14 39 Wang, Z. *et al.* Syngeneic animal models of tobacco-associated oral cancer reveal the activity
15 of in situ anti-CTLA-4. *Nat Commun* **10**, 5546, doi:10.1038/s41467-019-13471-0 (2019).
- 16 40 Bankhead, P. *et al.* QuPath: Open source software for digital pathology image analysis. *Sci
17 Rep* **7**, 16878, doi:10.1038/s41598-017-17204-5 (2017).
- 18 41 Borchert, N. *et al.* Proteogenomics of *Pristionchus pacificus* reveals distinct proteome
19 structure of nematode models. *Genome Res* **20**, 837-846, doi:10.1101/gr.103119.109 (2010).
- 20 42 Rappsilber, J., Mann, M. & Ishihama, Y. Protocol for micro-purification, enrichment, pre-
21 fractionation and storage of peptides for proteomics using StageTips. *Nat Protoc* **2**, 1896-
22 1906, doi:10.1038/nprot.2007.261 (2007).
- 23 43 Schmitt, M. *et al.* Quantitative Proteomics Links the Intermediate Filament Nestin to
24 Resistance to Targeted BRAF Inhibition in Melanoma Cells. *Mol Cell Proteomics* **18**, 1096-
25 1109, doi:10.1074/mcp.RA119.001302 (2019).
- 26 44 Theurillat, I. *et al.* Extensive SUMO Modification of Repressive Chromatin Factors
27 Distinguishes Pluripotent from Somatic Cells. *Cell Rep* **32**, 108146,
28 doi:10.1016/j.celrep.2020.108146 (2020).

- 1 45 Cox, J. & Mann, M. MaxQuant enables high peptide identification rates, individualized
2 p.p.b.-range mass accuracies and proteome-wide protein quantification. *Nat Biotechnol* **26**,
3 1367-1372, doi:10.1038/nbt.1511 (2008).
- 4 46 Cox, J. *et al.* Andromeda: a peptide search engine integrated into the MaxQuant environment.
5 *J Proteome Res* **10**, 1794-1805, doi:10.1021/pr101065j (2011).
- 6

1 **ACKNOWLEDGEMENTS**

2 We thank Dorothea Hillmann (Labormedizinisches Zentrum Dr. Risch) for her contributions to
3 laboratory analyses.

4

5 **Funding:** This research was supported by grants from the Swiss National Science Foundation
6 (PP00P3_157448 to L.F., P400PM_194473 to O.H.A.), the Research Fund of the Kantonsspital St.
7 Gallen (20/20 to L.F.), and the Promedica Foundation (1449/M to S.D.B.).

8

9 **Competing interests:** J.M.P. is founder and shareholder of Apeiron (Vienna, Austria), developing
10 soluble ACE2 as a COVID-19 therapy. J.M.P. has no direct competing interest relating to the paper or
11 data presented in the paper. All other authors have no competing interests to declare.

12

13 **Supplementary information** is available for this paper.

14

1 **FIGURE LEGENDS**

2 **Fig. 1: a**, Representative images of diffuse alveolar disease (DAD) from COVID-19 patients and non-
3 COVID-19 patients show hyaline membrane formation, desquamation and beginning of septal
4 fibrosis. Hematoxylin and eosin staining. **b**, RNA sequencing data of DAD resulting from COVID-19
5 (n=11) and other causes (n=10) reveals a clustered upregulation of genes. **c**, Gene set enrichment
6 analysis shows a significant correlation of the systemic lupus erythematosus enrichment pattern and
7 COVID-19 ($P=0.02$). A trend can be observed for autoimmune thyroid disease. **d**, Heatmap (center
8 panel) displaying fold-levels of autoantibodies (auto-Abs) relative to the upper reference limits of the
9 diagnostic laboratory assays, in descending order (left to right). The left panel shows autoimmune
10 diseases, while the right panel lists associated auto-Abs. The bottom panel indicates the individual
11 patients, with severe (marine blue, n=39) or asymptomatic (light blue, n=7) COVID-19.
12 Abbreviations: APS = antiphospholipid syndrome, RA = rheumatoid arthritis, SLE = systemic lupus
13 erythematosus, Vasc = vasculitis. **e**, Comparison of the cumulative autoimmunity scores derived from
14 the median value of each antibody. Patients with severe COVID-19 score (n=39) significantly higher
15 than asymptomatic patients (n=7, $P=0.02$). Score calculation is described in the Methods section.

16
17 **Fig. 2: a**, Indirect Immunofluorescence of lung tissue shows that IgA antibodies are present in diffuse
18 alveolar damage of COVID-19 patients. **b**, RNA-seq expression of type II pneumocytes, the main
19 producer of surfactant, shows abundant overexpression of surface proteins C (SFTPC), B (SFTPB),
20 A1 (SFTPA1) and A2 (SFTPA2). **c**, Immunofluorescence staining of lung tissue with serum from
21 severely ill COVID-19 patients shows co-localization of IgA binding with surfactant. Co-localization
22 of IgA and the target protein is visualized in the right lower graph.

23
24 **Fig. 3: a**, ELISA with poractant alfa (Curosurf®) demonstrates that significantly more IgA is binding
25 in plasma from severe COVID-19 (n=18) compared to asymptomatic patients (n=6; mean with 95%
26 CI, $P=0.006$). **b**, Mass spectrometry of poractant alfa lists abundance of surfactant binding proteins B
27 (SFTPB) and C (SFTPC). **c**, Pull-downs of poractant alfa reveal immunoglobulins binding to SFTPB
28 predominantly in severe COVID-19 samples. **d**, ELISA with recombinant proteins show that patients

1 with severe COVID-19 (n=18) have significantly more IgA against SFTPB ($P=0.001$) and
2 significantly more IgA against SFTPC ($P=0.004$) than asymptomatic patients (n=6) in the blood
3 (mean with 95% CI). **e**, Indirect immunofluorescence with healthy lung tissue indicates reduced
4 amounts of surfactant in non-COVID-19 diffuse alveolar damage (DAD) than in COVID-19 DAD.
5

Fig.1: COVID-19 patients with severe illness have a distinct mRNA expression pattern in damaged alveolar tissue and elevated autoantibodies in their blood.

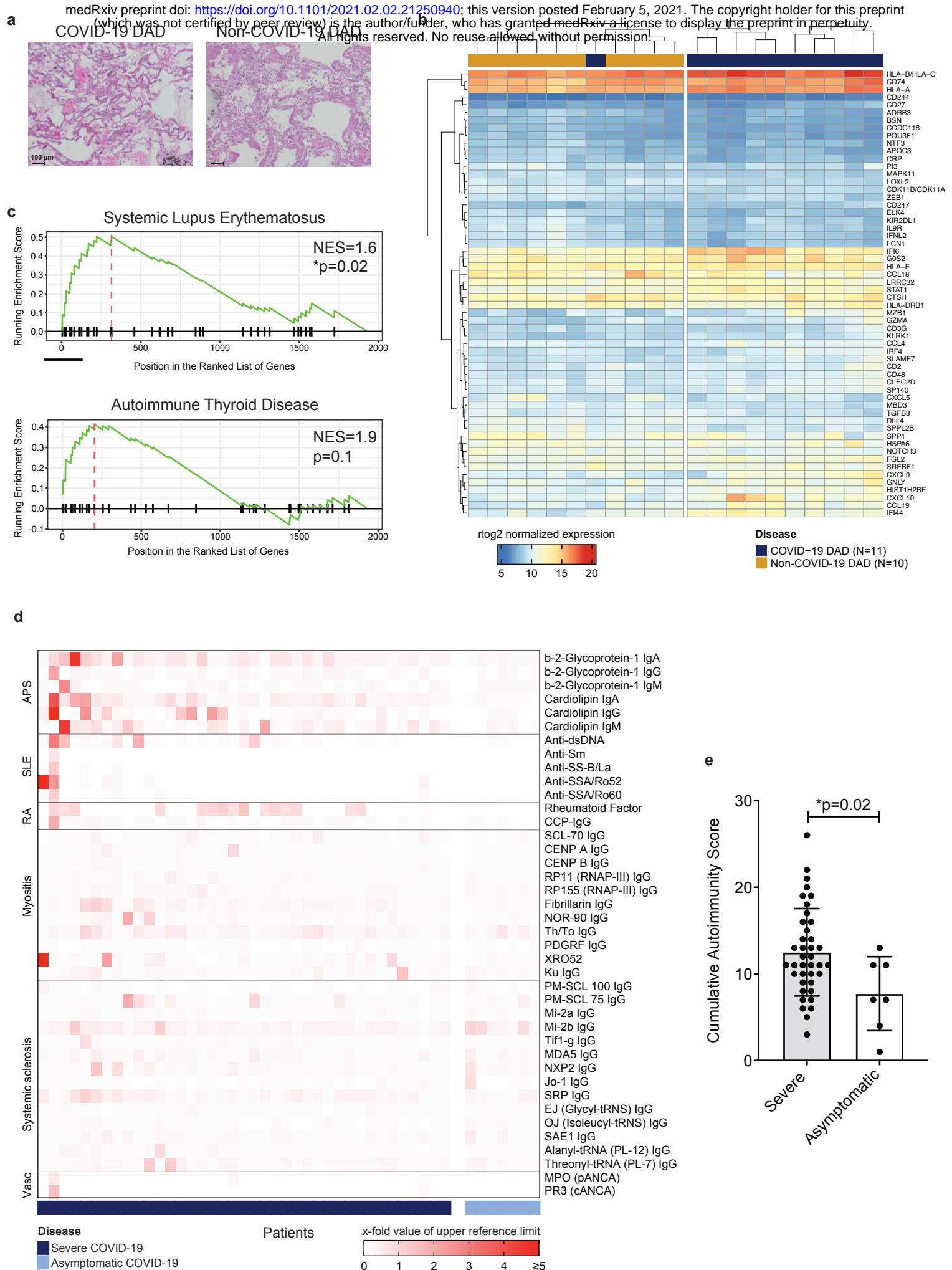


Fig. 2: Immunoglobulins of severe COVID-19 patients co-localize with surfactant in lung tissue.

medRxiv preprint doi: <https://doi.org/10.1101/2021.04.25.21050940>; this version posted February 15, 2021. The copyright holder for this preprint (which was not certified by peer review) is the author/funder, who has granted medRxiv a license to display the preprint in perpetuity.

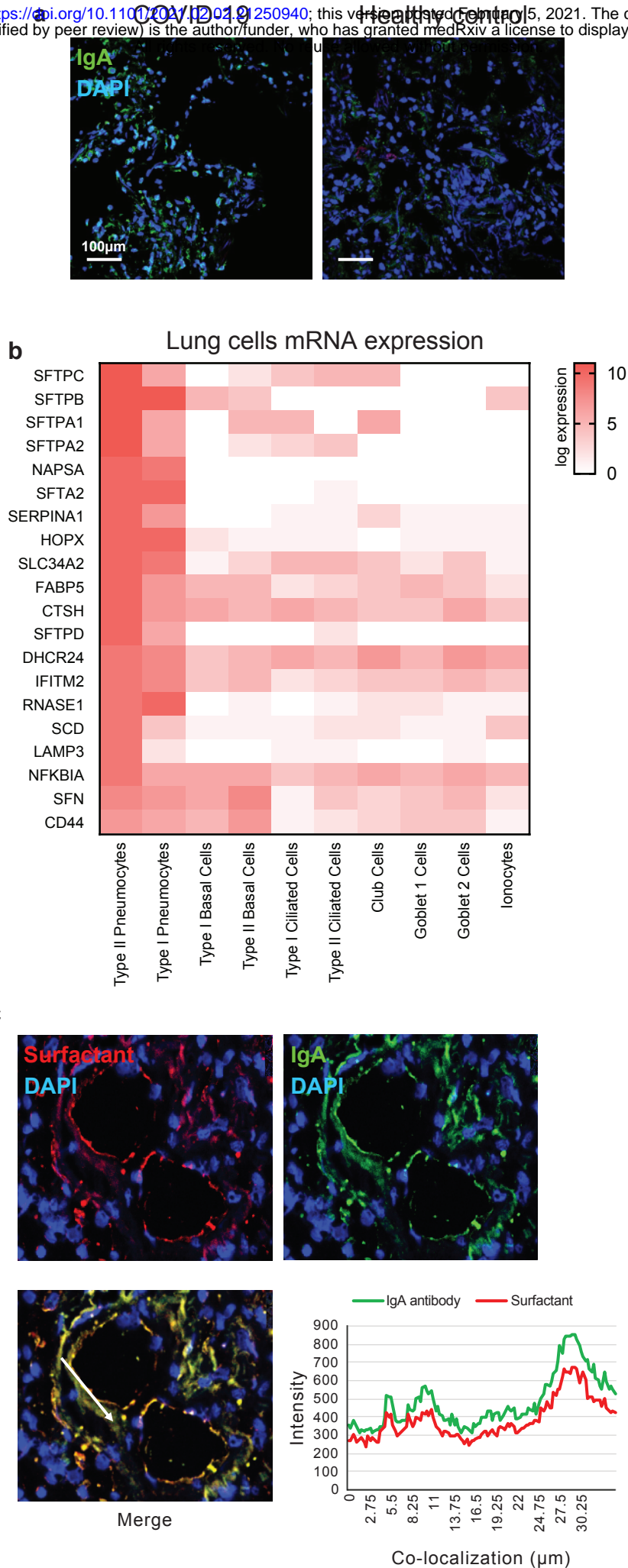


Fig. 3: Severe COVID-19 is associated with elevated IgA against surfactant proteins B and C, and shows diminished alveolar surfactant.

medRxiv preprint doi: <https://doi.org/10.1101/2021.02.02.21250940>; this version posted February 5, 2021. The copyright holder for this preprint (which was not certified by peer review) is the author/funder, who has granted medRxiv a license to display the preprint in perpetuity. All rights reserved. No reuse allowed without permission.

